JACS
JOURNAL OF THE AMERICAN CHEMICAL SOCIETY
Article
pubs.acs.org/JACS

How Water Fosters a Remarkable 5-Fold Increase in Low-Pressure CO_2 Uptake within Mesoporous MIL-100(Fe)

Estelle Soubeyrand-Lenoir,[†] Christelle Vagner,[†] Ji Woong Yoon,[#] Philippe Bazin,[‡] Florence Ragon,[§] Young Kyu Hwang,[#] Christian Serre,[§] Jong-San Chang,[#] and Philip L. Llewellyn*[,†]

[†]MADIREL (UMR CNRS 7246), Aix-Marseille University and CNRS, Centre de St Jerome, 13013 Marseille, France

[#]Research Group for Nanocatalyst, Korea Research Institute of Chemical Technology (KRICT), Yusung, Daejeon305-600, Republic of Korea

[‡]Laboratoire Catalyse et Spectrochimie (UMR CNRS 6506), ENSICAEN, Université de Caen and CNRS, 6 Bd Maréchal Juin, 14050 Caen, France

[§]Institut Lavoisier (UMR CNRS 8180), Université de Versailles St Quentin en Yvelines and CNRS, 45 avenue des Etats-Unis, 78035 Versailles, France

Supporting Information

ABSTRACT: The uptake and adsorption enthalpy of carbon dioxide at 0.2 bar have been studied in three different topical porous MOF samples, HKUST-1, UiO-66(Zr), and MIL-100(Fe), after having been pre-equilibrated under different relative humidities (3, 10, 20, 40%) of water vapor. If in the case of microporous UiO-66, CO_2 uptake remained similar whatever the relative humidity, and correlations were difficult for microporous HKUST-1 due to its relative instability toward water vapor. In the case of MIL-100(Fe), a remarkable 5-fold increase in CO_2 uptake was observed with increasing RH, up to 105 mg g^{-1} CO_2 at 40% RH, in parallel with a large decrease in enthalpy measured. Cycling measurements show slight differences for the initial three cycles and complete reversibility with further cycles. These results suggest an enhanced solubility of CO_2 in the water-filled mesopores of MIL-100(Fe).

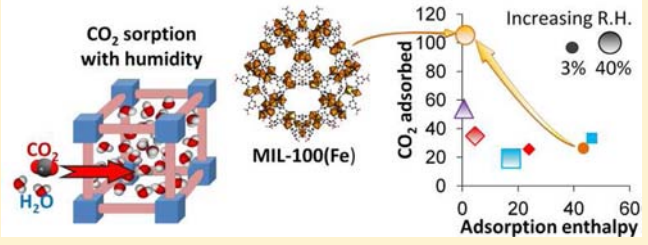

INTRODUCTION

There is no doubt that there is a global increase in land−sea temperatures with time.[1] While factors such as celestial variations[2] and stratospheric water vapor concentration[3] contribute to this temperature variation, it is clear that there is also a strong correlation of anthropogenic activities to global CO_2 levels. This sharp increase of CO_2 atmospheric concentration over recent times, as observed at Mauna Loa for example,[4] explains the huge effort devoted to CO_2 management.

Recovery of CO_2 from industrial processes is a challenging problem, with various technologies being investigated including amine baths,[5] membranes,[6] and chemical capture.[7] The use of adsorption with porous solids can also prove of interest. Indeed, pressure swing adsorption is a relatively economical and technically simple process for the separation or purification of specific components from a gas mixture. Thus, the search for materials with a high adsorption capacity, fast adsorption−desorption kinetics, and mild regeneration properties is ever continuing.

Several families of adsorbent materials are currently used in separation processes, including silicas, aluminas, zeolites, and active carbons.[8] More recently, other porous solids such as metal organic frameworks (MOFs)[9,10] have also shown promise in areas such as hydrogen storage,[11−13] recovery of greenhouse gases,[14−18] liquid phase separation,[19,20] energy storage,[21] and drug delivery.[22,23]

Significant amounts of water vapor can be present in some gas separation processes, and while in a limited number of cases water may aid the separation (3% of water is present in BaY for xylene separation, for example[24]), water is most often detrimental to separations. As an example, Brandani and Ruthven[25] investigated the effect of water on CO_2 adsorption on X zeolites and showed that the CO_2 adsorption capacity at a given partial pressure is strongly reduced by the presence of water. This adsorbed water essentially acts as a contaminant poison for many gases, including CO_2.

The effect of water on CO_2 uptake has only recently been studied in the case of MOFs.[26,27] Benchmark work by the group of Yazaydın et al. has shown that small amounts of water (4 wt %) may increase CO_2 uptake in HKUST-1 by 45% at 1 bar.[28] Yiu et al. also studied CO_2 uptake on HKUST-1 that was pre-equilibrated with different water loadings.[29] At low water loadings, the CO_2 capacity effectively increased by 10%, but with further increases in water loading the uptake of CO_2

Received: March 22, 2012
Published: May 16, 2012

   dx.doi.org/10.1021/ja302787x | J. Am. Chem. Soc. 2012, 134, 10174−10181

gradually fell. Cycling measurements also showed a decrease in CO_2 uptake, which was attributed to the partial degradation of the network. Decomposition of the HKUST-1 network at high relative humidity (RH) was also highlighted by Gul-E-Noor et al.[30] using ^1H and ^{13}C solid-state NMR. The structure was stable when only a small amount of water (0.5 mol equiv with respect to copper) was absorbed, but decomposition occurred at higher water contents. This instability of some MOFs in the presence of water has been studied by other groups,[31,32] although many other MOF structures have been shown to be water stable.[32,33]

Another material that has shown promise is the CPO-27 MOF. The high concentration of Lewis metal sites in this MOF profers an exceptional low-pressure capture of CO_2, which unfortunately decreases drastically in the presence of a limited amount (>4%) of water.[29]

Some of us have shown that the flexible MOF MIL-53(Cr) is found in the NP form when pre-equilibrated at 50% RH. In this state, only negligible methane uptake occurs up to 40 bar. In the case of CO_2, negligible uptake occurs up to 20 bar, at which point the NP→LP transition occurs and CO_2 is adsorbed with displacement of the pre-adsorbed water.[34] In the case of the mesoporous MOF MIL-100(Cr), water adsorbed on the Cr^{3+} CUS leads to an increased Brønsted acidity, as observed by FTIR.[35]

The present work has taken these various previous studies one step further. In the context of postcombustion CO_2 capture, a flow system was built in which a carrier gas (nitrogen), the target adsorptive (carbon dioxide at a pressure of 0.2 bar), and varying quantities of water vapor (3, 10, 20, and 40% RH) were allowed to flow through different MOF samples. The particularity of this system is that the sample is placed in a calorimeter, allowing direct measurement of the heat effects occurring at any time. Breakthrough curves were obtained with the aid of a gas chromatograph, and the water was further evaluated with a hygrometer. Various protocols were used to evaluate CO_2 uptake and the associated energy under different relative humidities. For one system, the CO_2 cycling experiments were carried out at two different relative humidities, and some initial FTIR studies were carried out. However, prior to this, the stability of the samples in the presence of water was investigated via a simple cycling of water vapor isotherms.

To highlight the different behaviors that can be observed with various MOFs, three topical systems were chosen for this study: UiO-66,[36] HKUST-1,[37] and MIL-100(Fe).[38] The UiO-66 material $[Zr_6O_4(OH)_4[O_2C\text{-}C_6H_4\text{-}CO_2]_6]$ is composed of zirconium oxoclusters which are linked through 12 terephthalate ligands.[36] Its cubic structure is built up from octahedral cages (diameter d = 11 Å) and eight tetrahedral cages (d = 7.5 Å) in a 1:2 ratio, accessible through triangular windows of a free diameter of 5−7 Å. UiO-66 is of interest here as it has been shown to be stable to quite high temperatures (above 480 °C[39]) as well as to humidity.

HKUST-1[37] [Cu-BTC, or $Cu_3(BTC)_2(H_2O)_3$] is one of the most studied MOFs to date. Its structure is built from copper paddlewheels related together through four benzene-1,3,5-tricarboxylate (BTC) linkers to create a 3D cubic pore system. This material presents a bimodal distribution of pores: a large central pore with d = 9.0 Å surrounded by pockets with d = 5.0 Å. Pores and pockets are interconnected by triangular windows with d = 3.5 Å. It has one of the highest volumetric uptakes of CO_2 (230 cm^3 cm^{-3} at 6 bar[40]) and was the sample highlighted by Liu et al.[29] for its increased CO_2 uptake in the presence of 4% water.

MIL-100(Fe)[38] $[Fe^{III}_3O(H_2O)_2X(C_6H_3(CO_2)_3)_2$ (X = F, OH)] was chosen as a mesoporous MOF with quite high molar CO_2 uptake (18 mmol g^{-1} at 50 bar[41]). Its 3D framework is constructed from hybrid supertetrahedral units consisting of inorganic subunits of trimers of iron(III) octahedra connected together by oxygen atoms from the organic linker BTC. Two types of mesoporous cages are created by the assembly of supertetrahedra with d = 25 and 29 Å, respectively, accessible through microporous windows of 4.7 × 5.5 and 8.6 Å. A significant amount of accessible Lewis iron(III) sites are accessible that can be partially reduced to iron(II) sites, resulting in higher interaction with specific gas molecules (NO, propylene, etc.).[35] It is this latter system which shows the most interesting results, and so both an FTIR study and cycling measurements were carried out in an attempt to elucidate further the mechanism of the CO_2 capture.

RESULTS AND DISCUSSION

Stability to Water Vapor Observed by Isotherm Cycling. Prior to the adsorption of CO_2 in the presence of humidity, pure water isotherms were obtained at 298 K on the three samples, and these isotherms were cycled six times without any further activation (Figure 1). In the case of UiO-66, a reversible stepped Type-V isotherm is obtained with significant water uptake around 20% RH. A slight loss of uptake (4%) occurs after the first run, which can be explained by a small rehydroxylation of the sample.[39] However, for the second to sixth runs, the water isotherms on this sample overlap, which indicates good water stability under these conditions. This does not seem to be the case for the HKUST-1 sample used here. Indeed, Type-I-shaped isotherms are obtained which are similar in shape to those observed previously.[31] However, for each of the water isotherm cycles, a slight decrease in uptake was observed to lead to >50% loss in volume during the sixth run. This loss in pore volume was confirmed by nitrogen physisorption experiments (see SI), and a certain loss in crystallinity of the sample exposed to water was also observed by XRD (see SI). In the case of MIL-100(Fe), Type-V-shaped isotherms are again measured with a marked hysteresis loop. This isotherm shape is similar to that observed previously.[31] The water uptake starts at 25% RH, and each of the six isotherms overlap, showing no sample degradation under these experimental conditions.

CO_2 Adsorption in the Presence of Water. *Uptakes and Energies.* A flow system was built on the laboratory scale to follow the effect of water on CO_2 adsorption. The experimental setup (see SI for details) is similar to those used in other studies,[29] with the exception that the sample was placed inside a Tian-Calvet microcalorimeter in order to directly follow the heat effects occurring during the experimental protocol. Breakthrough curves were obtained with a gas chromatograph, and the exited water was additionally followed with a hygrometer.

The approach taken in this study to follow the effect of water on CO_2 adsorption was to use a dynamic system at 1 bar with nitrogen as vector gas. CO_2 adsorption was carried out at a partial pressure of 0.2, chosen as being close to the partial pressure reached during some CO_2 emissions. The RH of the water vapor was varied at this fixed CO_2 partial pressure.

The protocol used here consists of three main steps, which are highlighted in Figure 2. The first step (region A in Figure 2)

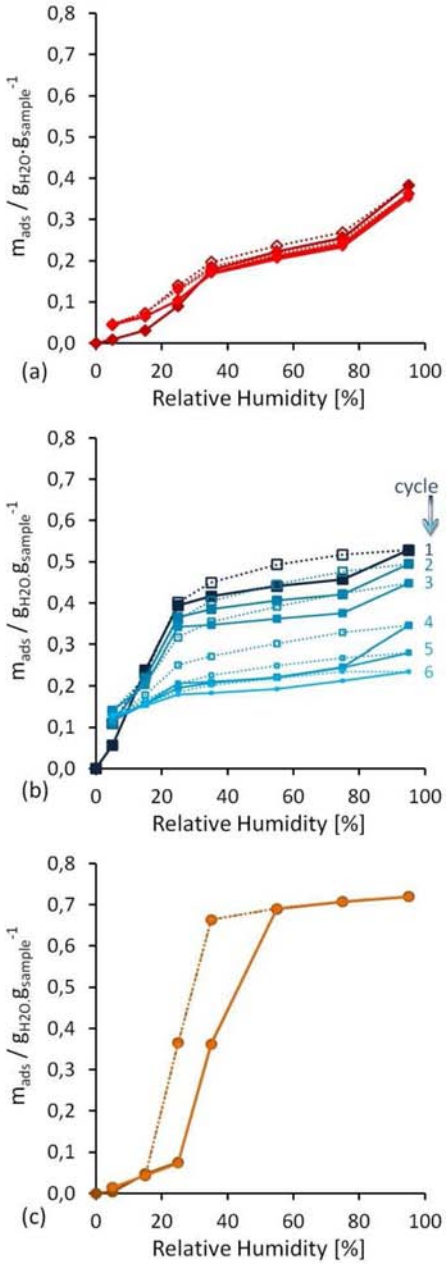

Figure 1. Water isotherm cycles carried out at 298 K on (a) UiO-66, (b) HKUST-1, and (c) MIL-100(Fe).

involves the adsorption−desorption of CO_2 on the sample to follow the reversibility of CO_2 adsorption. This reversibility can be followed from the breakthrough curves as well as from the microcalorimeter signal. The second step (region B in Figure 2) involves pre-equilibrating the sample with water vapor at the relative pressure chosen. After equilibration is attained, both CO_2 (0.2 partial pressure) and water vapor (at the given RH) are flowed through the sample. After this adsorption step, nitrogen is flowed through the sample in order to desorb both the water and the CO_2. Again the microcalorimeter signal allows a convenient way to estimate the degree of reversibility. The final step (region C in Figure 2) involves a second CO_2 adsorption−desorption cycle. This cycle can be compared to the first step in order to follow the reversibility/non-reversibility of the second step.

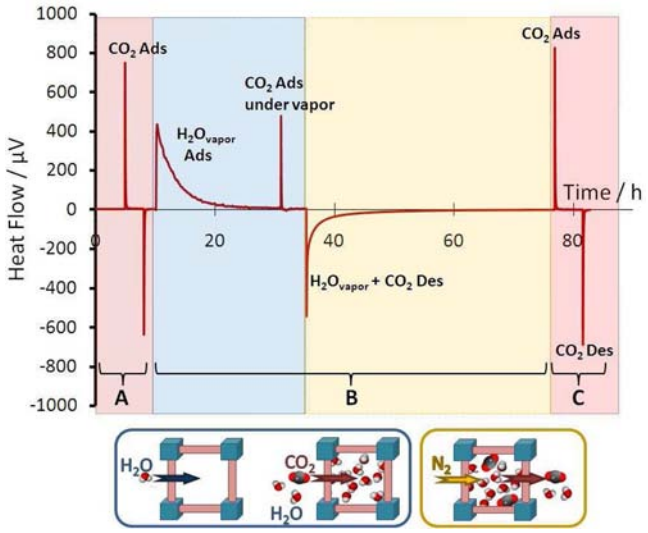

Figure 2. Heat flow curve obtained during an experiment showing the various steps in the experimental protocol.

Four series of experiments were thus carried out at water vapor relative humidities of 3, 10, 20, and 40%. Each experiment was repeated at least three times, and average values are reported. The results are presented in Figure 3 in bar graph form. The left-hand series shows CO_2 uptake as estimated from the breakthrough curve, whereas the right-hand graph shows the enthalpy associated with CO_2 uptake.

The uptake of CO_2 in the UiO-66 sample shows only minor differences under the various conditions of water vapor, and those can be considered to be within experimental error. The enthalpy signals observed during the adsorption of CO_2 in UiO-66 are also quite similar (range of −21 to −26 kJ mol^{-1}) for all the experiments, except for the adsorption of CO_2 at 40% RH. In comparison, the initial enthalpy of adsorption of pure CO_2 on the fully hydroxylated UiO-66 is around −25 to −26 kJ mol^{-1}.[39] The first adsorption sequences of CO_2 at all four relative humidities lie all in this region (−25 kJ mol^{-1}). When considering the second adsorption sequences in the presence of water vapor, a negligible difference in enthalpy is measured at 10% RH, whereas a slightly lower value of −21 kJ mol^{-1} is measured at 20% RH. Interestingly, an enthalpy of only −2 kJ mol^{-1} is recorded for the adsorption of CO_2 on UiO-66 at 40% RH. According to the pure water adsorption isotherm (Figures 1 and S1), the micropores of UiO-66 should be partially filled (to around 40%) with the vapor, and thus the pore-filling by CO_2 could occur with a concurrent displacement of water. Indeed, the hygrometer signal indicates water exiting from the cell. This measured enthalpy signal would thus be the overall result of an exothermic effect of CO_2 adsorption and an endothermic effect of water desorption. The third sequence, in pure CO_2, shows an enthalpy of −22 kJ mol^{-1}. This indicates that the previous desorption step removes a major part of the pre-adsorbed water reversibly. It would thus seem that, under the conditions chosen here, the uptake of CO_2 in UiO-66 is barely affected by the presence of water.

Adsorption of CO_2 on the HKUST-1 sample is more difficult to interpret. The uptake of CO_2 at 3% RH is around 35 mg g^{-1}, which is slightly below that measured on the same totally activated sample (40 mg g^{-1}),[42] although this difference may be due to differences in experimental approach. As observed previously,[29] an increase in amount of CO_2 adsorbed is

dx.doi.org/10.1021/ja302787x | J. Am. Chem. Soc. 2012, 134, 10174−10181

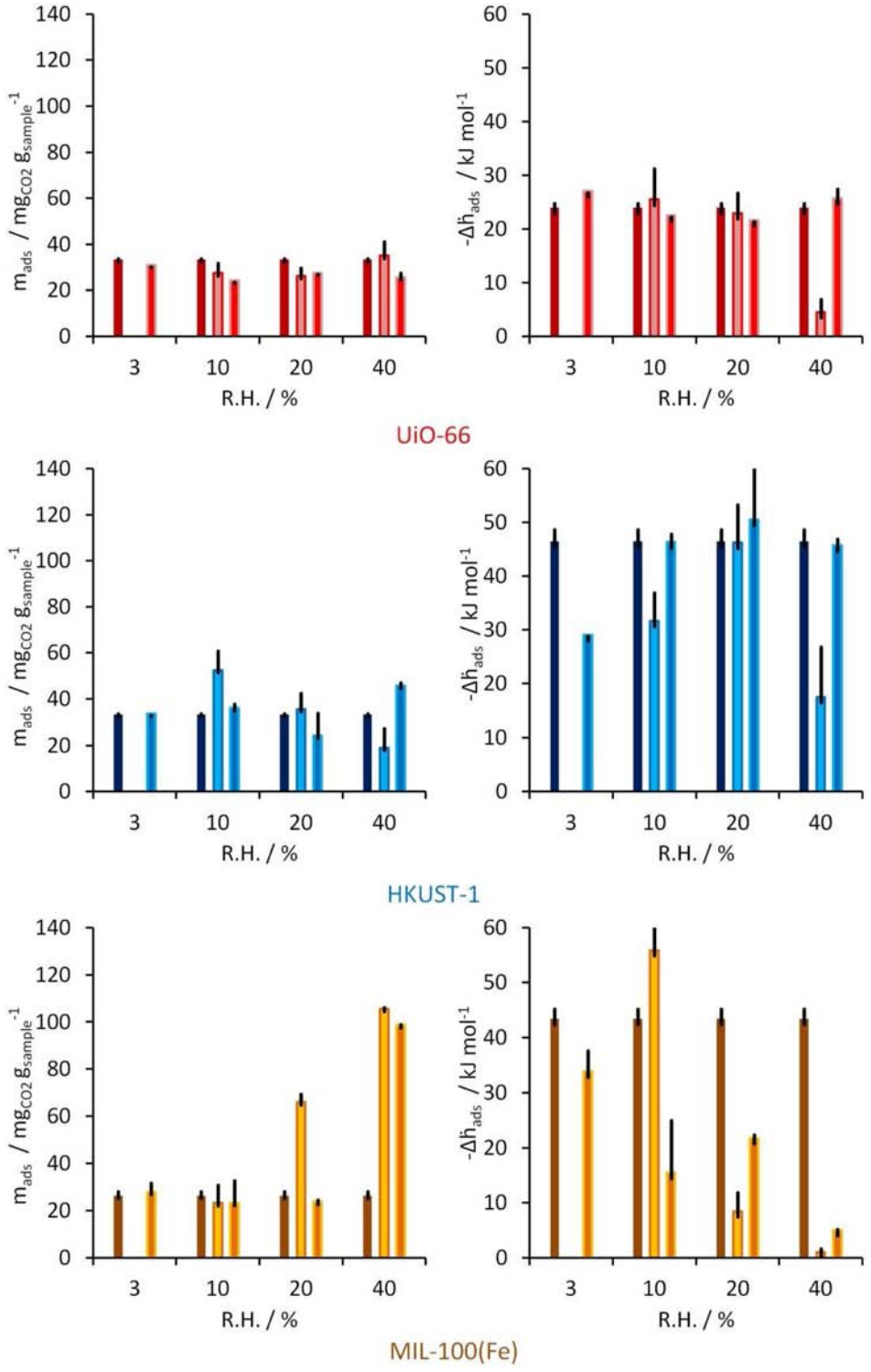

Figure 3. Dynamic CO_2 adsorption for UiO-66 (upper), HKUST-1 (middle), and MIL-100(Fe) (lower). Left: amounts of CO_2 adsorbed for various relative humidities. Right: corresponding adsorption enthalpies. Black bars show standard deviations. For each RH, the three bars correspond to CO_2 uptake during sequences A, B, and C in Figure 2.

observed in the presence of increased RH. Indeed, in the present case, at 10% RH, around 52 mg g^{-1} of CO_2 is adsorbed. However, further increases of RH to 20 and 40% lead to significant decreases in CO_2 adsorbed, to 41 mg g^{-1} and below 20 mg g^{-1}, respectively. It was noted during these experiments that the same sample could not be used for long periods. As for the pure water adsorption cycling experiments, partial sample degradation seems to occur, as highlighted by nitrogen uptake at 77 K on a sample obtained after the experiment carried out at 40% RH (see SI, Figure S2). The enthalpy of adsorption measured for CO_2 at 3% RH on the HKUST-1 sample was around −43 to −44 kJ mol^{-1}, well above that measured for pure CO_2 on the fully activated sample (−29 kJ mol^{-1}).[42] This highlights the role of water during this CO_2 uptake, which can

dx.doi.org/10.1021/ja302787x | J. Am. Chem. Soc. 2012, 134, 10174−10181

be explained reference to the work by Yazaydın et al.,[28] who suggested that water occupies the coordinatively unsaturated copper sites, inducing higher interactions with CO_2 with the protons of the water molecules. However, the enthalpies measured here are even higher than those proposed by Yazaydın et al. and this may be due to the simultaneous adsorption of both species. Note that the initial adsorption of pure water on HKUST-1 leads to enthalpy of around −95 kJ mol^{-1} (see SI, Figure S5). The initial adsorption of pure CO_2 leads to an enthalpy of around −29 kJ mol^{-1}.[42] If one considers that the enthalpy values measured here are a linear combination of the individual water and CO_2 enthalpy contributions, then it can be estimated that around 23% of this energy is due to water and the remaining 77% is due to the CO_2. At 10 and 20% RH, the adsorption enthalpies measured are around −31 and −33 kJ mol^{-1}, which are in the range predicted by Yazaydın et al.,[28] suggesting CO_2 adsorption on the hydrated, coordinatively unsaturated copper. The quite low enthalpy of adsorption measured at 40% RH can be explained by a concurrent displacement of water during the uptake of CO_2 (similar to the UiO-66/40% H_2O case). Thus, the overall results obtained with HKUST-1 agree with those of Yazaydın et al.[28] and Liu et al.[29] in which a small quantity of water seems to increase the uptake of CO_2 but at higher water vapor contents CO_2 uptake decreases. Slight differences in the explicit results are certainly due to the different samples used and the slightly different operating conditions.

The adsorption of CO_2 in the presence of humidity on the MIL-100(Fe) sample gives the most surprising results. At 3% RH, CO_2 uptake reaches 26 mg g^{-1} and corresponds to enthalpies of −43 and −34 kJ mol^{-1} for the repeated second run (Figure 3, right). These values can be compared to an uptake of around 22 mg g^{-1} and an associated enthalpy of −30 kJ mol^{-1} observed for pure CO_2.[41] Considering that the initial adsorption enthalpy of water on MIL-100(Fe) is around −80 kJ mol^{-1} (SI, Figure S6) and the initial enthalpy of CO_2 of −35 kJ mol^{-1},[41] this could be explained, as mentioned above for HKUST-1, by the simultaneous and independent adsorption of 14% of water and 82% of CO_2 on the coordinatively unsaturated iron sites. Alternatively, this value suggests that water adsorption on the CUS leads to stronger adsorption sites for CO_2, in agreement with the creation of an increased Brønsted acidity for MIL-100(Cr) upon coordination of water molecules on the Cr CUS.[35] During the second run at 3% RH, the enthalpy measured would suggest that only CO_2 is adsorbed and thus that all the CUS are saturated with water and/or CO_2. At 10% RH, a slight decrease in amount of CO_2 adsorbed on MIL-100(Fe) is observed which is accompanied by an enthalpy of around −56 kJ mol^{-1}. Interesting, at 20% RH around 66 mg g^{-1} of CO_2 is adsorbed, and surprisingly at 40% RH this reaches 105 mg g^{-1} of CO_2. Thus, under 40% RH, 5 times more CO_2 is adsorbed than under anhydrous conditions. Furthermore, the enthalpies of adsorption measured are around −8 and −1 kJ mol^{-1} for the adsorption at 20 and 40% RH, respectively. Again, these enthalpies can be explained by the concurrent displacement of water during CO_2 adsorption, which is further evidenced by the presence of water exiting from the cell, as observed by the hygrometer. These results of increased uptake, obtained from breakthrough experiments, are confirmed by direct gravimetric measurements at low pressure. Initial studies using FTIR suggest that water increasingly occupies the Brønsted sites in MIL-100(Fe) to the detriment of CO_2. This may therefore suggest that the formation of water induced increased Brønsted acidity at the Fe sites and migration/sorption of CO_2 to the center of the mesopores. This could not be confirmed by IR due the overlap of signals with those of the MOF structure, even though the presence of carbonates can be excluded. Indeed, the formation of carbonate species would be accompanied by large heat effects (the enthalpy of CO_2 chemisorption, forming carbonates, is >100 kJ mol^{-1}), which were not observed here.

This 5-fold increase in amount adsorbed associated with an almost athermal process is of great significance. An increase in CO_2 uptake in the presence of water is known to occur in other porous solids such as activated carbons. As an example, Wang et al.[43] reported a doubling of the amount of CO_2 adsorbed in the presence of water on a coconut shell carbon. This increase was explained by the formation of hydrates, and this effect was accompanied by an isosteric enthalpy of −63 kJ mol^{-1}. The authors further suggested that the enthalpy and hydrate formation varies as a function of pore size.[43] The concept of gas over-solubility has been suggested in the case of hydrogen adsorbed in mesoporous silicas and aluminas pre-equilibrated with *n*-hexane or ethanol.[44] In comparison with our study, this may suggest that it is possible to vary other parameters, including the pre-adsorbed fluid and adsorbing gas. Molecular modeling has been combined with experiments to understand the enhanced CO_2 solubility in hybrid adsorbents.[45−47] Here, a number of solid adsorbents have been considered, including MCM-41, SBA-15, alumina, activated carbon, silica gels, and zeolites. A number of confining fluids which are much bulkier than water were considered. In these studies, it was suggested that the CO_2 can adsorb in all of the pore volume due to confinement effects induced by the bulky molecules. It was also suggested that this phenomenon is less effective in the case of many microporous solids. This implies that an optimum in terms of pore size versus solvent size is required to gain an optimal packing density.

To summarize the present study with respect to this literature, even though increased uptake of CO_2 in porous samples pre-equilibrated with bulky molecular species has been observed or simulated for several materials, this is the first time that this has been evidenced to such a large extent in the case of MOF materials and with a simple pre-adsorbed species such as water. Indeed, while the increase in CO_2 uptake in HKUST-1 was theoretically suggested to reach 45%[28] and experimentally observed to be around 10%,[29] the MIL-100(Fe) system shows a 500% increase here.

It would seem, however, that one common feature of all these systems so far studied is the mesoporous architectures. Our work seems to suggest that the pre-equilibrated water in the mesoporous MIL-100(Fe) forms microporous pockets (Figure 4a) which are filled with CO_2 (Figure 4b) at lower pressures than if in the absence of water. However, it would seem that the CO_2 is able to displace some, but not all, of the water (Figure 4c). The more microporous systems such as zeolites or the UiO-66 studied here does not show any enhanced CO_2 uptake at low pressures in the presence of humidity. Indeed, this may be because the pre-adsorbed water does not produce any accessible microporosity (Figure 4d), even though in the case of UiO-66 it would seem that the CO_2 displaces some water (Figure 4e). This tentative explanation may be one step forward for eventually using this phenomenon in any real applications.

The CO_2 sorption results in the presence of the different RH's are summarized in Figure 5, where the amount of CO_2

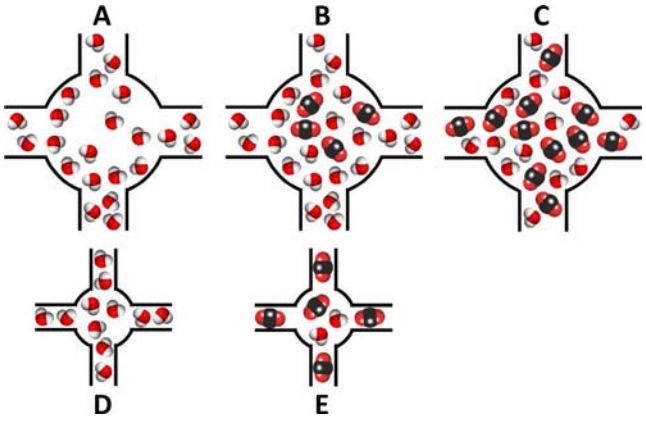

Figure 4. Schematic representation of possible mechanisms of CO_2 adsorption in the presence of humidity.

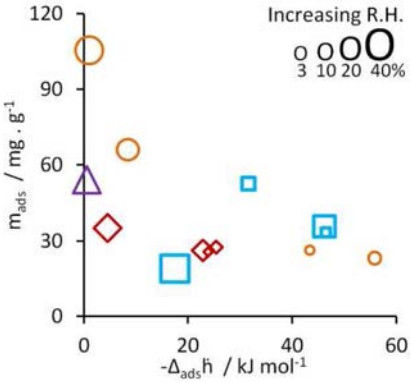

Figure 5. Amount of CO_2 adsorbed as a function of adsorption energy for the three MOF samples studied under the various RH's and compared with the zeolite NaX at 40% RH: ○, MIL-100(Fe); □, HKUST-1; ◇, UiO-66; △, NaX (increasing symbol size represents increasing RH).

adsorbed is plotted against the measured enthalpy. In such a graph, an ideal system can be expected to be found in the top left-hand region, with high uptake and low energy. We have included values that we obtained with a reference zeolite, NaX, obtained at 40% RH. In terms of uptake, Figure 5 indeed highlights the relatively constant CO_2 uptake with varying RH for UiO-66, the increase and subsequent decrease in CO_2 uptake with increasing RH for HKUST-1, and the very large increase in CO_2 uptake with increasing RH for MIL-100(Fe). The comparison with NaX is quite revealing. At 3% RH, an uptake of around 221 mg g^{-1} is observed (not shown), which is much higher than for any of the MOFs considered here. Indeed, it would seem that only the CPO-27 materials[48] (Table 1) are able to take up such quantities of CO_2 at 0.2 bar. However, under 40% RH, a 4-fold decrease in CO_2 uptake is observed for NaX (54 mg g^{-1}),[48] which is only half of that observed for the MIL-100(Fe) sample at the same RH content. This decrease in CO_2 uptake with increasing RH is in agreement with the observations of Brandani and Ruthven for the Faujasite-type zeolites.[25] The enthalpies obtained with NaX equally show a large decrease, from −47 to −1 kJ mol^{-1}. This latter value suggests again concomitant water desorption on CO_2 uptake. The decrease in measured enthalpy at high RH for all of the MOF samples is also evident from Figure 5.

This underlines the high interest for the MIL-100(Fe) system under 40% RH. The CO_2 uptake of 105 mg g^{-1} at 40% RH can be compared to values found in the literature for uptake of pure CO_2 at 0.2 bar on different materials (see Table 1). It can be seen that this uptake is above that measured on the active carbon, is similar to that obtained with NaX, and is below half of that obtained with the two different CPO-27 samples. Note, however, that the enthalpies of adsorption for the NaX and the CPO-27 samples are above −40 kJ mol^{-1}, and these heat effects are significant when developing an adsorption-based process. Furthermore, as stated above, both the zeolite and CPO-27 lose their CO_2 sorption properties in the presence of water due to poisoning of the cation/metal sites. It is further suggested that the CPO-27 samples are not highly stable in the presence of humidity, as is also the case for the HKUST system.

Table 1. Comparison of Reported Data for Pure CO_2 Uptake at 0.2 bar for Different Materials and Their Initial Adsorption Enthalpy

sample	CO_2 uptake/mg g^{-1}	enthalpy/kJ mol^{-1}
UiO-66	27[37]	−25−26[37]
HKUST-1	40[40]	−28[40]
MIL-100(Fe)	22[39]	−30[39]
CPO-27(Mg)	260[46]	−43[46]
CPO-27(Ni)	220[46]	−39[46]
Takeda 5A	31[a]	−26[a]
NaX	177[a]	−54[a]

[a]In-house measurements.

Cycling the MIL-100(Fe) System. CO_2 uptake during several cycles in the presence of either 3 or 40% RH was evaluated in the case of the most interesting MIL-100(Fe) system. Figure 6 shows the uptake and corresponding enthalpy for several cycles.

For both relative humidities studied, a decrease in CO_2 uptake occurs for the first cycles until a plateau is reached in each case. At 3% RH, this plateau is reached after around four runs, with an approximate 20% decrease in amount adsorbed. The adsorption energies also decrease from around −44 to −33 kJ mol^{-1}, suggesting an increased role of the water vapor. However, for all of the six cycles, the desorption energy does not match that of adsorption, suggesting that full reversibility is not attained.

At 40% RH, a 36% decrease in CO_2 uptake is observed after 3 runs before a steady-state regime seems to be attained where the adsorption−desorption energies are equivalent. The CO_2 uptake in this steady-state regime of around 70 mg g^{-1} is still above many MOFs, and the combination of significant amount adsorbed vs low adsorption energy is still of interest for further investigation.

■ CONCLUSIONS

Low-pressure CO_2 uptake (0.2 bar) has been analyzed for three topical microporous or mesoporous MOFs pre-equilibrated with water vapor. For the first time, a remarkable enhancement of CO_2 uptake through pre-adsorption of water vapor has been highlighted here in the case of mesoporous MIL-100(Fe). This may arise from the coordination of water molecules on the Lewis metal sites, while adsorption of CO_2 occurs in the center of the pores with no carbonate formation. The system can be cycled reversibly after 2−3 initial equilibration cycles. The measured enthalpies are remarkably low for the systems pre-equilibrated with 40% RH, suggesting a partial desorption of water on CO_2 sorption.

The key properties of the MIL-100(Fe) system seem to be its stability under these conditions and the presence of

dx.doi.org/10.1021/ja302787x | J. Am. Chem. Soc. 2012, 134, 10174−10181

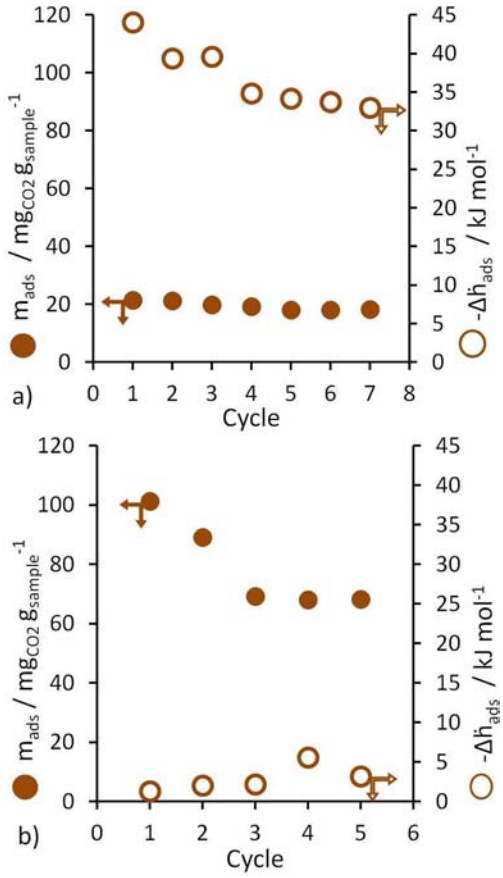

Figure 6. Amount adsorbed (full circles) and corresponding enthalpy (open circles) obtained during the CO_2 cycling experiments on MIL-100(Fe) for (a) 3 and (b) 40% RH.

mesoporosity. Indeed, HKUST-1 was shown to degrade in the presence of humidity, and UiO-66 did not show any enhanced uptake. On comparing with other materials in which enhanced CO_2 uptake in confined media has been suggested, mesoporosity seems to be a common factor.

This study provides an opening to further investigations. The presence of water vapor in a process no longer seems to be a limiting factor for CO_2 recovery at low pressures, as would be the case for zeolites, for example. The low enthalpies measured suggest that limited heat effects in a column bed and CO_2 uptake during cycling are comparable or better with respect to other materials. As such, this work marks a significant step in the problem of low-pressure CO_2 recovery.

■ ASSOCIATED CONTENT

Supporting Information

Discussion and data regarding MOFs synthesis, pure water sorption isotherm, nitrogen adsorption at 77 K, room-temperature sorption under dynamic conditions, microcalorimetry at ambient temperature, and CO_2 adsorption/desorption cycles. This material is available free of charge via the Internet at http://pubs.acs.org.

■ AUTHOR INFORMATION

Corresponding Author

philip.llewellyn@univ-amu.fr

Notes

The authors declare no competing financial interest.

■ ACKNOWLEDGMENTS

The research leading to these results has received funding from the European Community's Seventh Framework Programme (FP7/2007−2013) under grant agreement no. 228862 (Macademia project). This work was also financially supported by the KCRC, funded by MEST, and through the CNRS international scientific collaboration program (PICS).The authors thank Alexander Vimont for fruitful discussions. E.S.-L., C.V., and P.L.L. thank Sandrine Bourrelly, Renaud Denoyel, Dominique Vincent, and Yvan Cecere for technical assistance. J.-S.C., Y.K.H., and J.W.Y. thank You-Kyong Seo for experimental assistance.

■ REFERENCES

(1) Hansen, J.; Ruedy, R.; Sato, M.; Lo, K. *Rev. Geophys.* **2010**, *48*, RG4004.
(2) Scafetta, N. *J. Atm. Solar-Ter. Phys.* **2010**, *72*, 951.
(3) Solomon, S.; Rosenlof, K. H.; Portmann, R. W.; Daniel, J. S.; Davis, S. M.; Sanford, T. J.; Plattner, G.-K. *Science* **2010**, *327*, 1219.
(4) http://www.esrl.noaa.gov/gmd/ccgg/trends/
(5) Sander, M. T.; Mariz, C. L. *Ener. Conv. Man.* **1992**, *33*, 341.
(6) Pennline, H. W.; Luebke, D. R.; Jones, K. L.; Myers, C. R.; Morsi, B. I.; Heintz, Y. J.; Ilconich, J. B. *Fuel Proc. Tech.* **2008**, *89*, 897.
(7) Choi, S.; Drese, J. H.; Jones, C. W. *Chem. Sus. Chem.* **2009**, *2*, 796.
(8) Yang, R. T. *Gas separation by adsorption processes*; Imperial College Press: London, 1997.
(9) Férey, G. *Chem. Soc. Rev.* **2008**, *37*, 191.
(10) Kitagawa, S.; Kitaura, R.; Noro, S.-I. *Angew.Chem. Int. Ed.* **2004**, *43*, 2334.
(11) Latroche, M.; Surblé, S.; Serre, C.; Mellot-Draznieks, C.; Llewellyn, P. L.; Lee, J.-H.; Chang, J.-S.; Jhung, S. H.; Férey, G. *Angew. Chem., Int. Ed.* **2006**, *45*, 8227.
(12) Liu, Y.; Eubank, J. F.; Cairns, A. J.; Eckert, J.; Kravtsov, V. C.; Luebke, R.; Eddaoudi, M. *Angew. Chem., Int. Ed.* **2007**, *46*, 3278.
(13) Li, Y.; Yang, R. T. *Langmuir* **2007**, *23*, 12937.
(14) Férey, G.; Serre, C.; Devic, T.; Maurin, G.; Jobic, H.; Llewellyn, P. L.; De Weireld, G.; Vimont, A.; Daturi, M.; Chang, J.-S. *Chem. Soc. Rev.* **2011**, *40*, 550.
(15) Keskin, S.; van Heest, T. M.; Sholl, D. S. *Chem. Sus. Chem.* **2010**, *3*, 879.
(16) Hamon, L.; Llewellyn, P. L.; Devic, T.; Ghoufi, A.; Clet, G.; Guillerm, V.; Pirngruber, G. D.; Maurin, G.; Serre, C.; Driver, G.; Beek, W. v.; Jolimaître, E.; Vimont, A.; Daturi, M.; Férey, G. *J. Am. Chem. Soc.* **2009**, *131*, 17490.
(17) Furukawa, H.; Yaghi, O. M. *J. Am. Chem. Soc.* **2009**, *131*, 8875.
(18) Sumida, K.; Rogow, D. L.; Mason, J. A.; McDonald, T. M.; Bloch, E. D.; Herm, Z. R.; Bae, T. H.; Long, J. R. *Chem. Rev.* **2012**, *112*, 724.
(19) Alaerts, L.; Maes, M.; Giebeler, L.; Jacobs, P. A.; Martens, J. A.; Denayer, J. F. M.; Kirschhock, C. E. A.; De Vos, D. E. *J. Am. Chem. Soc.* **2008**, *130*, 14170.
(20) Maes, M; Trekels, M; Boulhout, M; Schouteden, S; Vermoortele, F; Alaerts, L; Heurtaux, D; Seo, Y. K.; Hwang, Y. K.; Chang, J.-S.; Beurroies, I; Denoyel, R; Temst, K; Vantomme, A; Horcajada, P; Serre, C; De Vos, D. E. *Angew. Chem., Int. Ed.* **2011**, *50*, 4210−4214.
(21) Beurroies, I.; Boulhout, M.; Llewellyn, P. L.; Kuchta, B.; Férey, G.; Serre, C.; Denoyel, R. *Angew. Chem., Int. Ed.* **2010**, *49*, 7526.
(22) Horcajada, P.; Chalati, T.; Serre, C.; Gillet, B.; Sebrie, C.; Baati, T.; Eubank, J. F.; Heurtaux, D.; Clayette, P.; Kreuz, C.; Chang, J.-S.; Hwang, Y. K.; Marsaud, V.; Bories, P.-N.; Cynober, L.; Gil, S.; Férey, G.; Couvreur, P.; Gref, R. *Nat. Mater.* **2010**, *9*, 172.
(23) Horcajada, P.; Gref, R.; Baati, T.; Allan, P. K.; Maurin, G.; Couvreur, P.; Férey, G.; Morris, R. E.; Serre, C. *Chem. Rev.* **2012**, *112*, 1232−1268.

(24) Hotier, G.; Pucci, A.; Methivier, A. Patent FR2757507(A1), 1998.
(25) Brandani, F.; Ruthven, D. M. *Ind. Eng. Chem. Res.* **2004**, *43*, 8339.
(26) Kizzie, A. C.; Wong-Foy, A. G.; Matzger, A. J. *Langmuir* **2011**, *27*, 6368.
(27) Liu, J.; Benin, A. I.; Furtado, A. M. B.; Jakubczak, P.; Willis, R. R.; LeVan, M. D. *Langmuir* **2011**, *27*, 11451.
(28) Yazaydın, A. O.; Benin, A. I.; Faheem, S. A.; Jakubczak, P.; Low, J. J.; Willis, R. R.; Snurr, R. Q. *Chem. Mater.* **2009**, *21*, 1425.
(29) Liu, J.; Wang, Y.; Benin, A. I.; Jakubczak, P.; Willis, R. R.; LeVan, M. D. *Langmuir* **2010**, *26*, 14301.
(30) Gul-E-Noor, F.; Jee, B.; Poppl, A.; Hartmann, M.; Himsl, D.; Bertmer, M. *Phys. Chem. Chem. Phys.* **2011**, *13*, 7783.
(31) Küsgens, P.; Rose, M.; Senkovska, I.; Fröde, H.; Henschel, A.; Siegle, S.; Kaskel, S. *Microporous Mesoporous Mater.* **2009**, *120*, 325.
(32) Low, J. J.; Benin, A. I.; Jakubczak, P.; Abrahamian, J. F.; Faheem, S. A.; Willis, R. R. *J. Am. Chem. Soc.* **2009**, *131*, 15834.
(33) Mu, B.; Walton, K. S. *J. Phys. Chem. C* **2011**, *115*, 22748.
(34) Llewellyn, P. L.; Bourrelly, S.; Serre, C.; Filinchuk, Y.; Férey, G. *Angew. Chem., Int. Ed.* **2006**, *45*, 7751.
(35) Leclerc, H.; Vimont, A.; Lavalley, J.-C.; Daturi, M.; Wiersum, A. D.; Llwellyn, P. L.; Horcajada, P.; Férey, G.; Serre, C. *Phys. Chem. Chem. Phys.* **2011**, *13*, 11748.
(36) Cavka, J. H.; Jakobsen, S.; Olsbye, U.; Guillou, N.; Lamberti, C.; Bordiga, S.; Lillerud, K. P. *J. Am. Chem. Soc.* **2008**, *130*, 13850.
(37) Chui, S. S.-Y.; Lo, S. M.-F.; Charmant, J. P.; nbsp, H.; Orpen, A. G.; Williams, I. D. *Science* **1999**, *283*, 1148.
(38) Horcajada, P.; Surblé, S.; Serre, C.; Hong, D.-Y.; Seo, Y.-K.; Chang, J.-S.; Grenèche, J.-M.; Margiolaki, I.; Férey, G. *Chem. Commun.* **2007**, 2820.
(39) Wiersum, A. D.; Soubeyrand-Lenoir, E.; Yang, Q.; Moulin, B.; Guillerm, V.; Ben Yahia, M.; Bourrelly, S.; Vimont, A.; Miller, S.; Vagner, C.; Daturi, M.; Clet, G.; Serre, C.; Maurin, G.; Llewellyn, P. L. *Chem.—Asian J.* **2011**, *6*, 3270.
(40) Chowdhury, P.; Bikkina, C.; Meister, D.; Dreisbach, F.; Gumma, S. *Microporous Mesoporous Mater.* **2009**, *117*, 406.
(41) Yoon, J. W.; Seo, Y.-K.; Hwang, Y. K.; Chang, J.-S.; Leclerc, H.; Wuttke, S.; Bazin, P.; Vimont, A.; Daturi, M.; Bloch, E.; Llewellyn, P. L.; Serre, C.; Horcajada, P.; Grenèche, J.-M.; Rodrigues, A. E.; Férey, G. *Angew. Chem., Int. Ed.* **2010**, *49*, 5949.
(42) Grajciar, L. S.; Wiersum, A. D.; Llewellyn, P. L.; Chang, J.-S.; Nachtigall, P. *J. Phys. Chem. C* **2011**, *115*, 17925.
(43) Wang, Y.; Zhou, Y.; Liu, C.; Zhou, L. *Colloids Surf. A* **2008**, *322*, 14.
(44) Rakotovao, V.; Ammer, R.; Miachon, S.; Pera-Titus, M. *Chem. Phys. Lett.* **2010**, *485*, 299.
(45) Ho, N. L.; Porcheron, F.; Pellenq, R. J.-M. *Langmuir* **2010**, *26*, 13287.
(46) Ho, N. L.; Perez Pellitero, J.; Porcheron, F.; Pellenq, R. J.-M. *Langmuir* **2011**, *27*, 8187.
(47) Ho, N. L.; Perez Pellitero, J.; Porcheron, F.; Pellenq, R. J.-M. *J. Phys. Chem. C* **2012**, *116*, 3600−3607.
(48) Dietzel, P. D. C.; Besikiotis, V.; Blom, R. *J. Mater. Chem.* **2009**, *19*, 7362.